

On the late spectral types of cataclysmic variable secondaries

I. Baraffe¹ and U. Kolb²

¹ *Ecole Normale Supérieure de Lyon, C.R.A.L. (UMR 5574 CNRS), F-69364 Lyon Cedex 07, France (ibaraffe@ens-lyon.fr)*

² *Department of Physics & Astronomy, The Open University, Walton Hall, Milton Keynes, MK7 6AA (u.c.kolb@open.ac.uk)*

Submitted to MNRAS: 15 February 2000

ABSTRACT

We investigate why the spectral type of most cataclysmic variable (CV) secondaries is significantly later than that of a ZAMS star with the same mean density. Using improved stellar input physics, tested against observations of low-mass stars at the bottom of the main sequence, we calculate the secular evolution of CVs with low-mass donors. We consider sequences with different mass transfer rates and with a different degree of nuclear evolution of the donor prior to mass transfer.

Systems near the upper edge of the gap ($P \sim 3\text{--}6$ h) can be reproduced by models with a wide range of mass transfer rates from $1.5 \times 10^{-9} M_{\odot}\text{yr}^{-1}$ to $10^{-8} M_{\odot}\text{yr}^{-1}$. Evolutionary sequences with a small transfer rate and donors that are substantially evolved off the ZAMS (central hydrogen content 0.05 – 0.5) reproduce CVs with late spectral types above $P \gtrsim 6$ h. Systems with the most discrepant (late) spectral type should have the smallest donor mass at any given P .

Consistency with the period gap suggests that the mass transfer rate increases with decreasing donor mass for evolved sequences above the period gap. In this case, a single-parameter family of sequences with varying X_c and increasing mass transfer rate reproduces the full range of observed spectral types. This would imply that CVs with such evolved secondaries dominate the CV population.

Key words: novae, cataclysmic variables — stars: evolution — stars: low-mass — binaries: close

1 INTRODUCTION

Over last two decades, numerous studies have considered the evolution of the low-mass secondaries in cataclysmic variable (CV) systems. The calculations aimed mainly at reproducing the observed distribution of orbital periods P of CVs, in particular the minimum period at 80 min and the dearth of systems in the 2-3 h period range (see e.g. King 1988 for a review). Based on the most popular explanation for this period gap, the disrupted magnetic braking model (cf. Rappaport, Verbunt and Joss 1983; Spruit and Ritter 1983), evolutionary sequences constructed with full stellar models or simplified bipolytrope models (cf. Hameury et al. 1988; Hameury 1991; Kolb and Ritter 1992; and references therein) reproduce the broad features of the observed P distribution. Despite the significant uncertainties in the underlying stellar input physics (e.g. opacities, equation of state, etc...), the lack of a reliable description of angular momentum losses \dot{J} that drive the mass transfer provided sufficient freedom that it was always possible to find a set of secondary star models which reasonably fit the period gap.

Input physics like atmospheric opacities and the outer

boundary condition are essential for a comparison with observable quantities such as colours or spectral types.

The spectral type and the orbital period ($P \propto (R^3/M)^{1/2}$; R and M are the secondary radius and mass) provide a unique set of constraints that test the structure both of the secondary's interior and its outermost layers. As we shall show below, these can be used to find constraints on the actual orbital braking strength \dot{J} as well.

Previously, an analysis of this kind was hampered by the lack of knowledge, both theoretical and observational, of stars in the low-mass range populated by CV secondaries. Here we make use of the marked and independent progress in the study of low-mass stars over the past decade. A wealth of ground-based and space-based observations has significantly improved our knowledge of the photometric and spectroscopic properties of stars at the bottom of the main sequence. In parallel, recent theoretical work has demonstrated the necessity to use accurate internal physics and outer boundary conditions based on non-grey atmosphere models to correctly describe the structure and evolution of low-mass objects (Burrows et al. 1993; Baraffe et al. 1995, 1997, 1998; Chabrier and Baraffe 1997, 2000, and references

therein). These interior models, combined with recent, much improved models of cool atmospheres and synthetic spectra (see the review of Allard et al. 1997, and references therein) allow one to calculate self-consistent magnitudes and synthetic colours of low-mass stars. These can be compared directly to observed quantities, avoiding the use of uncertain empirical effective temperature T_{eff} and bolometric correction scales. The agreement between models and observations for (i) eclipsing binary systems (Chabrier and Baraffe 1995), (ii) mass-magnitude and mass-spectral type relations (Baraffe and Chabrier, 1996; Chabrier et al. 1996), (iii) colour-magnitude diagrams (Baraffe et al. 1997, 1998) and (iv) synthetic spectra (Leggett et al. 1996; Allard et al. 1997), demonstrate how reliable the theory of low-mass stars already is.

Recently, Beuermann et al. (1998) used our preliminary calculations based on these next-generation low-mass star models and compared calculated and observed spectral types (SpT) of CV secondaries. Beuermann et al. (1998) found that CVs with donors that are nuclearily evolved, with a substantial amount of central hydrogen depletion, can account for the late spectral types in long-period systems ($P/h \gtrsim 6$), but not in those close to the upper edge of the period gap ($3 \lesssim P/h \lesssim 6$). Higher mass transfer rates as usually assumed can account for the latter.

The purpose of the present paper is to give a detailed account of the full set of our CV evolutionary calculations, a preliminary subset of which has been used by Beuermann et al. 1998. We discuss implications of the need for both high mass transfer rates and a significant fraction of systems with nuclearily evolved donors. We focus on CVs where the spectral type can be determined fairly accurately, i.e. on systems with orbital period above 3 h. In a previous paper (Kolb and Baraffe 1999), we considered aspects specific to the evolution of systems below the period gap ($P \leq 2$ h).

In §2 we summarize the input physics and present evolutionary sequences with initial ZAMS donors. Nuclearily evolved sequences are presented in §3. A discussion and conclusions follow in §4.

2 EVOLUTIONARY MODELS WITH INITIAL ZAMS DONOR

A brief description of the input physics for our stellar code can be found in Kolb and Baraffe (1999) and Baraffe et al. (1998). More details are given by Chabrier and Baraffe (1997) for the interior physics and by Hauschildt et al. (1999) for the atmosphere models. Here we just recall the main improvements compared to earlier models applied to CV donors: (i) the new models are based on the equation of state (EOS) of Saumon et al. (1995) which is specially devoted to low-mass stars and brown dwarfs, and to the description of strong non-ideal effects characterizing the interior stellar plasma; (ii) the outer boundary condition is based on non-grey atmosphere models (the use of a grey boundary condition overestimates the effective temperature T_{eff} and luminosity L for a given mass M); (iii) mass-colour and mass-magnitude relations are derived self-consistently from the synthetic spectra of the same atmosphere models which provide the boundary condition.

We use the empirical SpT - ($I - K$) relation estab-

lished by Beuermann et al. (1998) to determine the spectral type SpT for a given model (M, T_{eff}, L) from the calculated colour $I - K$. The accuracy and relevance of this conversion is discussed in Beuermann et al. (1998).

Because of the uncertainty of current descriptions for orbital angular momentum losses by magnetic braking and the substantial computer time (cf. Kolb and Ritter, 1990; Hameury 1991) required for evolutionary sequences if mass transfer is treated explicitly and self-consistently, we restrict our analysis to sequences calculated with constant mass transfer rate. We have checked that sequences with mass transfer driven by angular momentum losses \dot{J} with either constant \dot{J} , constant \dot{J}/J , or \dot{J} according to Verbunt & Zwaan (1981), have the same main properties as the sequences with constant \dot{M} on which we base our conclusions.

In this section we consider sequences where mass transfer starts with donors of mass $M_2 = 1M_{\odot}$ that are initially on the ZAMS, with solar composition ($X = 0.70$, $Z=0.02$). We define a “standard sequence” which reproduces the width and location of the period gap (2.1 - 3.2 h) in the framework of the disrupted magnetic braking model. This sequence is calculated with $\dot{M} = 1.5 \times 10^{-9} M_{\odot} \text{yr}^{-1}$ until the donor becomes fully convective at $M_2 = 0.21 M_{\odot}$ and $P = 3.2$ h. At this point mass transfer ceases and the secondary shrinks back to its thermal equilibrium configuration in $2 - 3 \times 10^8$ years. Mass transfer resumes when the Roche lobe radius catches up with the donor radius at a period $P = 2.1$ h. The transfer rate in this second phase is $5 \times 10^{-11} M_{\odot} \text{yr}^{-1}$, a value typical for systems driven by gravitational wave emission (cf. Kolb and Baraffe 1999). This standard sequence is shown in Fig. 1 (thick solid line), together with sequences calculated with higher transfer rates ($3 \times 10^{-9} M_{\odot} \text{yr}^{-1}$, $10^{-8} M_{\odot} \text{yr}^{-1}$ and $10^{-7} M_{\odot} \text{yr}^{-1}$).

Mass-losing stars deviate from thermal equilibrium. The deviation is large if the secondary’s thermal timescale $t_{\text{KH}} \sim GM^2/RL$ is long compared to the mass transfer timescale $t_M = M/(-\dot{M})$. As shown in Fig. 2a, mass transfer causes a contraction of the donor radius (e.g. Whyte and Eggleton 1980; Stehle et al. 1996) relative to the corresponding ZAMS radius for predominantly radiative objects $M \gtrsim 0.6M_{\odot}$, where the radiative core exceeds 80% of the total mass (cf. Chabrier and Baraffe 1997, their Fig. 9). Predominantly convective stars ($M \lesssim 0.6M_{\odot}$) expand relative to the ZAMS. Although a large mass transfer rate causes a significant departure of R from its equilibrium value (see Fig. 2a), Fig. 2b shows that T_{eff} is rather insensitive to \dot{M} (see also Singer et al. 1993; Kolb et al. 2000).

The outer boundary condition of the stellar model is more important than \dot{M} for the determination of T_{eff} , as indicated by the dotted curve in Fig. 1 and Fig. 2b. This curve corresponds to a sequence with $\dot{M} = 1.5 \times 10^{-9} M_{\odot} \text{yr}^{-1}$, but calculated with the Eddington approximation, which implicitly assumes greyness and the diffusion approximation for radiative transfer in the atmosphere. Chabrier and Baraffe (1997) have shown that such an approximation overestimates T_{eff} for a given mass when molecules form in the atmosphere at $T_{\text{eff}} \lesssim 4000 - 4500$ K. Note that the Eddington approximation sequence reproduces the period gap as well as the corresponding non-grey sequence, with a width and location of 2.2 - 3 h. However, the Eddington sequence consistently gives earlier spectral types than observed, and dramatically fails to reproduce the location of objects with

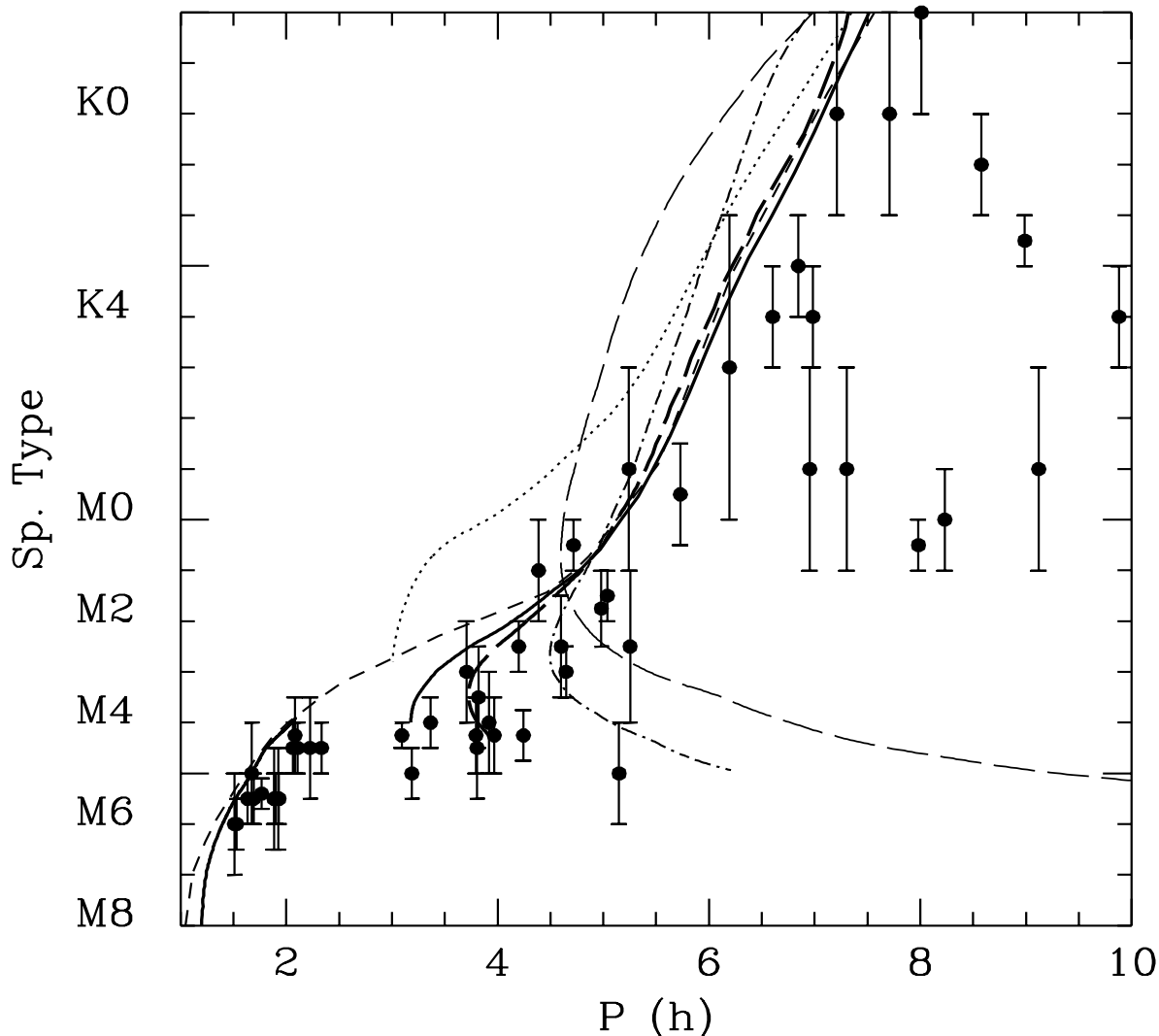


Figure 1. Spectral type of CV secondaries versus orbital period, for evolutionary tracks with unevolved donor stars and different mass transfer rate. The observed data are taken from Beuermann et al. (1998), with slight updates. The short-dashed curve corresponds to solar metallicity stellar models on the ZAMS. The thick solid curve is the standard sequence with constant $\dot{M} = 1.5 \times 10^{-9} M_{\odot} \text{yr}^{-1}$ above the period gap and $\dot{M} = 5 \times 10^{-11} M_{\odot} \text{yr}^{-1}$ below the gap. The thick long-dashed curve is with constant $\dot{M} = 3 \times 10^{-9}$; the dash-dotted curve is with $\dot{M} = 10^{-8} M_{\odot} \text{yr}^{-1}$; the thin long-dashed curve is with $\dot{M} = 10^{-7} M_{\odot} \text{yr}^{-1}$. For all sequences, the initial secondary mass is $M_2 = 1 M_{\odot}$. Sequences above the period gap terminate when the donor becomes fully convective. The dotted curve corresponds to a sequence with $\dot{M} = 1.5 \times 10^{-9} M_{\odot} \text{yr}^{-1}$, but calculated with the Eddington approximation as outer boundary condition for the stellar models.

$P \leq 5$ h in Fig. 1. This example highlights the significant improvements of our new generation of low-mass star models.

Note that the period P_{turn} where the period derivative changes from negative to positive due to departure from thermal equilibrium increases with mass transfer rate. Remarkably, the standard sequence reaches period bounce at $P = 3.2$ h, the same period where the secondary star becomes fully convective. Sequences with higher mass transfer rate bounce before the donor becomes fully convective. In other words, for mass transfer rates $\dot{M} \geq 1.5 \times 10^{-9} M_{\odot} \text{yr}^{-1}$,

the minimum period reached by CVs just corresponds to or exceeds the observed upper edge of the period gap at ~ 3 h.

As mentioned in Beuermann et al. (1998), a large spread of the secular mean mass transfer rates from $1.5 \times 10^{-9} M_{\odot} \text{yr}^{-1}$ to $\sim 10^{-8} M_{\odot} \text{yr}^{-1}$ could account for the observed range of late spectral type objects with $P \lesssim 5$ h. It is well known that such a spread of \dot{M} in systems above the period gap cannot be excluded by observations (cf. e.g. Warner 1995, his Fig. 9.8; Sproats et al. 1996).

Although the sharp observed gap boundaries seem to imply uniform values of the secular mean \dot{M} near the upper

Table 1. Donor mass M and mass M_{core} of its radiative core, at $P = 3$ h for evolved sequences with initial donor mass $M_2 = 1$ or $1.2 M_{\odot}$, constant mass transfer $\dot{M} = 1.5 \times 10^{-9} M_{\odot} \text{yr}^{-1}$ and different central H abundance X_c at the time mass transfer starts. t_0 is the age of the donor when mass transfer turns on.

M_2/M_{\odot}	X_c	t_0 (Gyr)	M/M_{\odot}	$M_{\text{core}}/M_{\odot}$
1	0.55	2.37	0.191	0.064
	0.16	7.2	0.209	0.125
	0.05	8.16	0.199	0.136
1.2	0.16	3.75	0.183	0.120
	0.05	4.18	0.143	0.127

edge of the period gap (e.g. Ritter 1996), a spread of \dot{M} cannot be dismissed unambiguously. The sharp upper edge is preserved if disrupted magnetic braking holds and \dot{M} adopts only values $\geq 1.5 \times 10^{-9} M_{\odot} \text{yr}^{-1}$. With increasing \dot{M} the critical mass where the secondary becomes fully convective becomes smaller (cf. Fig. 2a). Thus, if the system detaches at this point, by analogy with the disrupted magnetic braking model, mass transfer resumes after the secondary has reached thermal equilibrium at a period shorter than 2 h. As an example, for the sequence with $\dot{M} = 10^{-8} M_{\odot} \text{yr}^{-1}$ the donor becomes fully convective at $M_2 \sim 0.15 M_{\odot}$, and the system reappears as CV at $P \sim 1.7$ h. Test calculations with a population synthesis code (e.g. Kolb 1993) show that such a spread of systems reappearing below the gap still gives a reasonably sharp lower edge of the period gap, with only a mild over-accumulation of systems in a period interval 1.7–2.1 h. This is perfectly consistent with the observed distribution which does show a slight, although statistically probably not significant, accumulation of systems there.

Despite this consistency, accepting the \dot{M} spread is not an attractive solution to the late SpT problem. It is hard to see why a presumably global angular momentum loss mechanism should drive such different transfer rates in otherwise similar systems.

Finally we note that there are no CV secondaries above the ZAMS line in the P –SpT diagram for periods longer than ~ 6 h. This suggests that in these systems the secular mean \dot{M} must be smaller than $10^{-8} M_{\odot} \text{yr}^{-1}$. But whatever the value of \dot{M} , sequences with unevolved donors never drop below the ZAMS line for $P \gtrsim 6$ h.

3 EVOLVED SEQUENCES

We now consider sequences with initial donors which have evolved off the ZAMS prior to mass transfer. When mass transfer turns on, the star is old enough (cf. Table 1) to have burned a substantial amount of hydrogen in the centre. Only stars with mass $M > 0.35 M_{\odot}$, which develop a radiative core (cf. Chabrier and Baraffe 1997), start to deplete central H within a Hubble time. But only if $M > 0.8 M_{\odot}$ is more than 50% of the initial H depleted in less than 10 Gyr. Therefore, this donor type is restricted to systems that form with a fairly massive secondary $\gtrsim 1 M_{\odot}$.

Figure 3 depicts sequences with such nuclearily evolved donors — hereafter “evolved sequences” — in the P –SpT diagram, for different central H mass fractions X_c at the time mass transfer starts. The initial secondary mass is $M_2 =$

$1 M_{\odot}$ or $M_2 = 1.2 M_{\odot}$ and mass transfer rate is fixed to $1.5 \times 10^{-9} M_{\odot} \text{yr}^{-1}$. Table 2 gives for each of these sequences the secondary mass M , spectral type, T_{eff} and radius R as a function of P , for $3 \leq P/h \leq 10$. The evolutionary track of ZAMS donor sequences in the P –SpT diagram is insensitive to the initial donor mass, while for evolved sequences with the same initial X_c T_{eff} decreases (the spectral type becomes later) at a given P with increasing initial donor mass. This is illustrated in Fig. 3 where we plot sequences starting with $M_2 = 1 M_{\odot}$ (long-dashed curve) and $M_2 = 1.2 M_{\odot}$ (dash-dotted curve), both for $X_c = 0.05$.

As already emphasized by Beuermann et al. (1998), evolved sequences result in later spectral types for a given $P \gtrsim 5$ h than the standard sequence and can explain amazingly well the spread of data observed above 6 h. The reason for this is illustrated in Figures 4 and 5, which display several diagnostic quantities along the sequences as a function of secondary mass (Fig. 4) and orbital period (Fig. 5).

When mass transfer turns on, more evolved donors with smaller X_c have larger R , T_{eff} and T_c than less evolved donors. This follows from the well known properties of the H burning phase of solar-type stars with a central radiative core: as hydrogen is depleted in the centre, the increase of the central molecular weight μ yields an increase of the central temperature and thus L , causing an expansion of the star. Hence the main-sequence evolution of a star with constant mass proceeds towards larger L and T_{eff} . The same effect exists for mass-losing main-sequence stars. Consequently, for a given mass, R is larger for more evolved sequences, and P is longer, while for a given P , the secondary mass and T_{eff} is smaller, hence the spectral type is later (cf. Fig. 3). As a consequence, the donor mass at any given P is smallest for the most evolved sequence, cf. Table 2.

Although the evolved sequences shown in Fig 3 provide an attractive explanation for the observed data above 5-6 h, they are obviously in conflict with the standard explanation of the period gap. Indeed, with the adopted value $\dot{M} = 1.5 \times 10^{-9} M_{\odot} \text{yr}^{-1}$ we find that these sequences enter the period gap before the donor becomes fully convective or before the system bounces due to departure from thermal equilibrium. Table 1 gives the mass of the secondary and the mass M_{core} of its radiative core at $P = 3$ h for the different sequences. Period bounce occurs for the ($M_2 = 1 M_{\odot}$, $X_c = 0.16$) sequence at $P = 2.60$ h, corresponding to $M = 0.1 M_{\odot}$ and $M_{\text{core}} = 0.04 M_{\odot}$. The donor becomes fully convective only at $M \sim 0.05 M_{\odot}$ ($P = 2.9$ h). For more evolved sequences, period bounce would occur at even smaller periods.

This difference in the size of the radiative core is caused by the small central H abundance. The smaller X_c and the higher central temperature of evolved donors compared to unevolved donors (cf. Figs. 4 and 5) imply lower radiative opacities in the central region, and consequently favour radiative transport. As a result, the inward progression of the bottom of the donor’s convective envelope as mass decreases proceeds at a slower rate. Hence in evolved sequences the donor has a larger radiative core M_{core} than a donor with the same mass in an unevolved sequence (see Fig. 4). In terms of P , Fig. 5 shows that M_{core} is larger for the standard sequence at any given $P \gtrsim 3.5$ h. The situation then reverses at the upper edge of the gap, which corresponds to $M_{\text{core}} = 0$ for the standard sequence. The effect of a lower

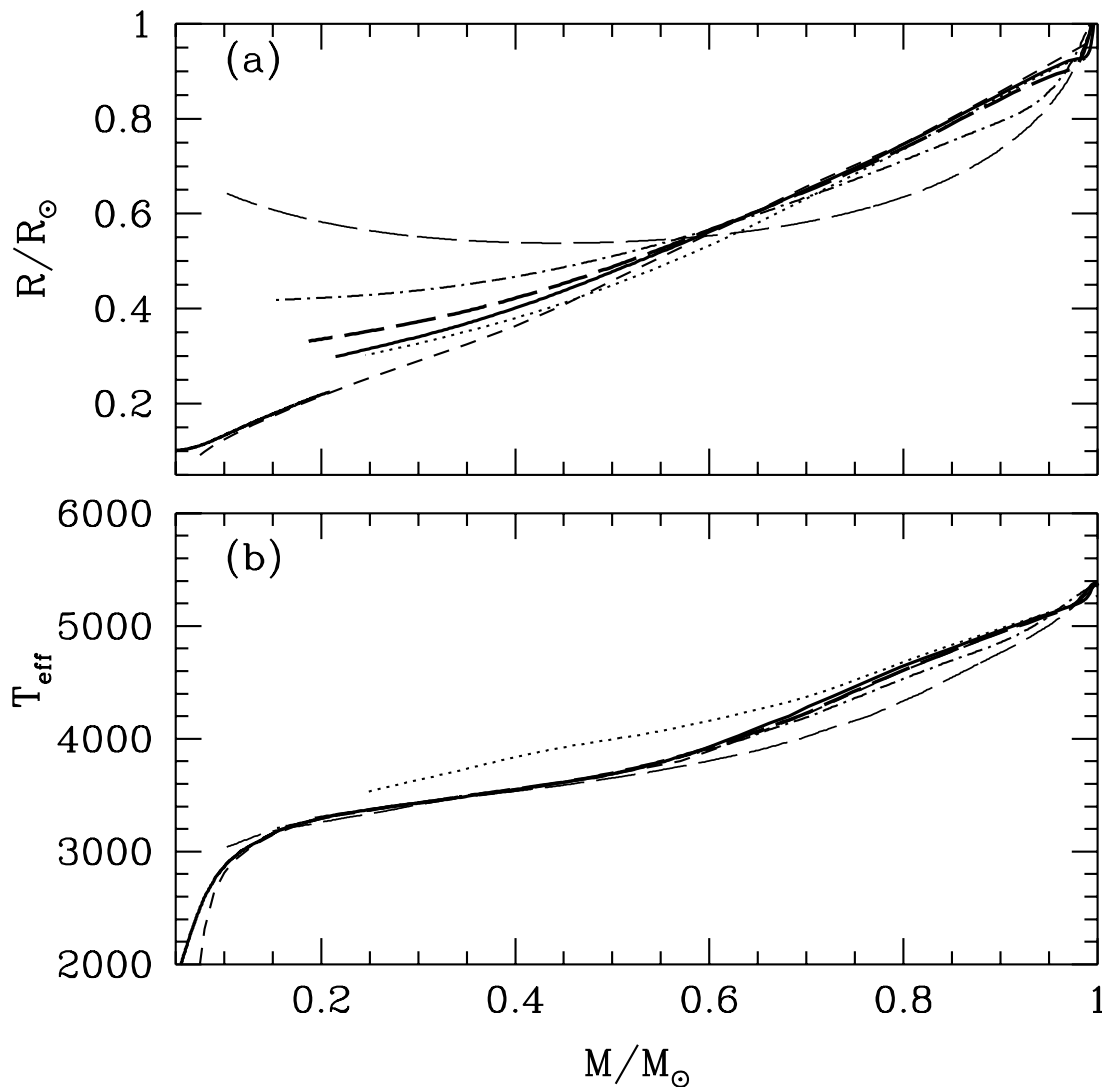


Figure 2. (a) Mass – radius relation for ZAMS stars and for unevolved CV donors in sequences with constant mass transfer rate. Linestyle as in Fig. 1. (b) Mass – T_{eff} relation for the same models as in (a).

central H abundance described above is similar to that reported by Laughlin et al. (1997) who followed the central H burning phase of very low-mass stars with $M \leq 0.25M_{\odot}$ (with constant mass). They note that stars which are fully convective on the ZAMS develop a radiative core towards the end of the main sequence because of the depletion of H and subsequent lowering of the central radiative opacities.

The P -SpT diagram suggests that at long orbital periods a fairly large fraction of systems has a significantly evolved donor. If these carried on evolving with a transfer rate $\simeq 1.5 \times 10^{-9} M_{\odot} \text{yr}^{-1}$ they would clearly overpopulate the period gap regime. This is made worse by the fact that some of these sequences reach their minimum period in the period gap (Fig. 3): at period bounce $\dot{P} = 0$, and the detection probability $d \propto 1/\dot{P}$ increases sharply. We find a similar behaviour if mass transfer is treated self-

consistently, with an angular momentum loss rate $\dot{J} = \text{const.}$ or $\dot{J} \propto J$, calibrated such that the corresponding unevolved sequence reproduces the observed period gap (giving $\dot{M} = 1.5 \times 10^{-9} M_{\odot} \text{yr}^{-1}$ at $P \sim 3$ h).

An obvious way to prevent evolved sequences from evolving into the period gap region is to increase the mass transfer rate. This increases the deviation from thermal equilibrium and leads to period bounce above the upper edge of the observed gap. Test calculations with constant mass transfer rate show that period bounce occurs at $P > 3$ h with $\dot{M} \geq 3 \times 10^{-9}$ and $5 \times 10^{-9} M_{\odot} \text{yr}^{-1}$ for sequences with respectively $X_c = 0.16$ and 0.05 , for initial donor mass $1M_{\odot}$. The same behavior is found for donors with higher initial mass. In other words, for sequences with smaller X_c a higher \dot{M} near the upper edge of the period gap is required than for less evolved donors, consistent with the fact that

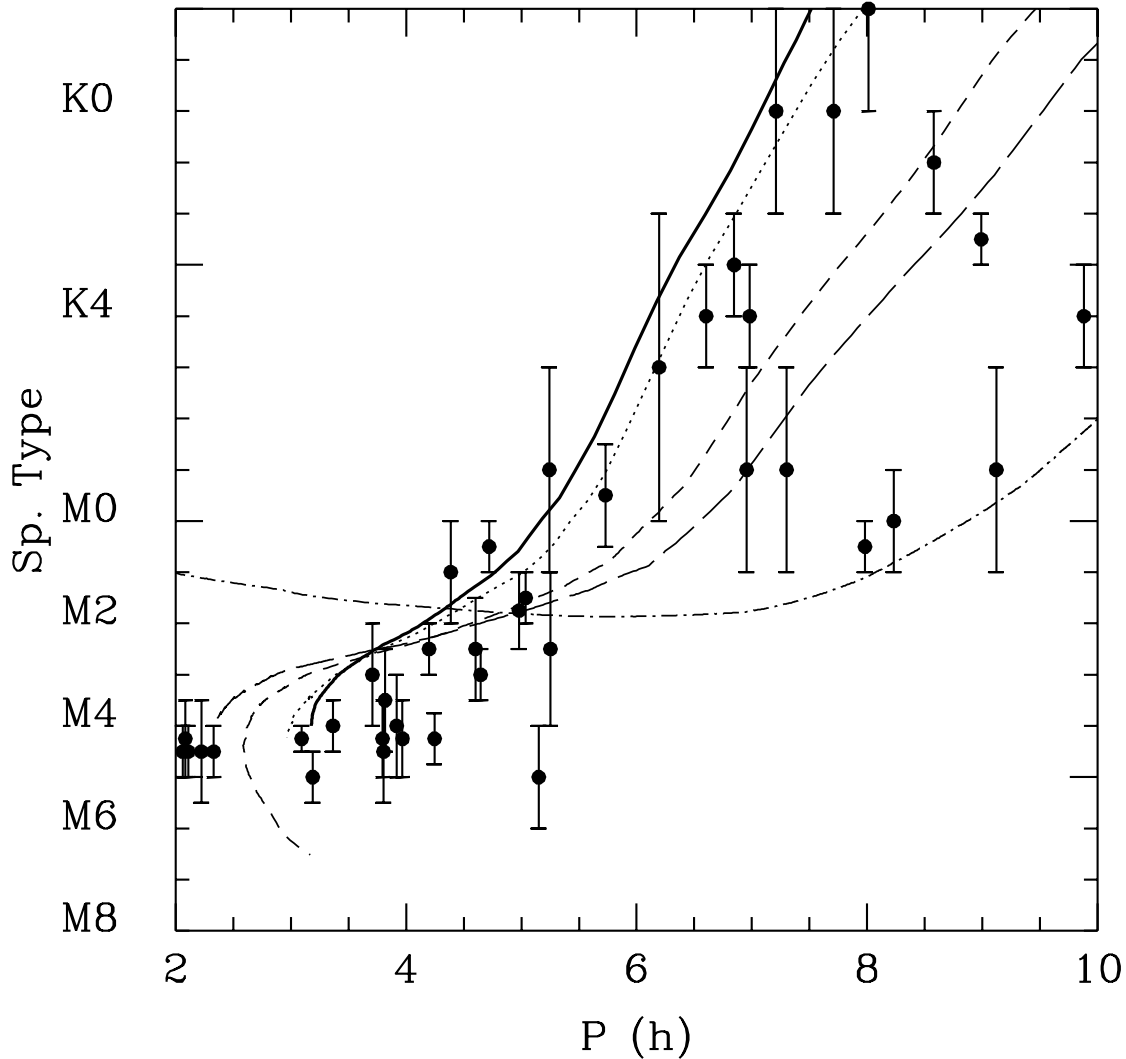


Figure 3. As Fig. 1, but for sequences with different initial central H abundance X_c at the time mass transfer starts. The mass transfer rate is $\dot{M} = 1.5 \times 10^{-9} M_{\odot} \text{yr}^{-1}$, the initial secondary mass $M_2 = 1$ and $1.2 M_{\odot}$. Thick solid line: standard sequence with $M_2 = 1 M_{\odot}$ and $X_c = 0.7$; dotted curve: $M_2 = 1 M_{\odot}$ and $X_c = 0.55$; dashed curve: $M_2 = 1 M_{\odot}$ and $X_c = 0.16$; long-dashed curve: $M_2 = 1 M_{\odot}$ and $X_c = 0.05$; dash-dotted curve: $M_2 = 1.2 M_{\odot}$ and $X_c = 0.05$. The data are the same as in Fig. 1.

the thermal time is shorter if X_c is small. These evolved sequences with high transfer rates ($\dot{M} > 5 \times 10^{-9} M_{\odot} \text{yr}^{-1}$) also match the observed spectral types in the region $P = 3$ -6 h, just as high \dot{M} sequences with ZAMS donors do (see §2 and Fig. 1).

Note however, that for long periods $P \gtrsim 5$ h a higher \dot{M} has the same effect as for the unevolved sequences discussed in §2 (Fig. 1). The effective temperature is larger and therefore the spectral type earlier than for a sequence with smaller \dot{M} . Thus in order to account for the full range of rather cool spectral types at long periods, \dot{M} cannot always be high along all evolved sequences.

To summarize: evolved sequences require high \dot{M} ($\gtrsim 5 \times 10^{-9}$) near the upper gap region to avoid crossing the

gap, but a low mass transfer rate ($\dot{M} \lesssim 5 \times 10^{-9}$) for $P \gtrsim 6$ h to explain the late spectral type CVs in this region. This suggests that the mean mass transfer rate increases during the secular evolution of nuclear evolved donors.

4 DISCUSSION AND CONCLUSIONS

We performed calculations of the long-term evolution of CVs with up-to-date stellar models that fit observed properties of single low-mass stars exceptionally well. Our focus was on the orbital period–spectral type (P –SpT) diagram, and the observed location of CV secondaries which populate

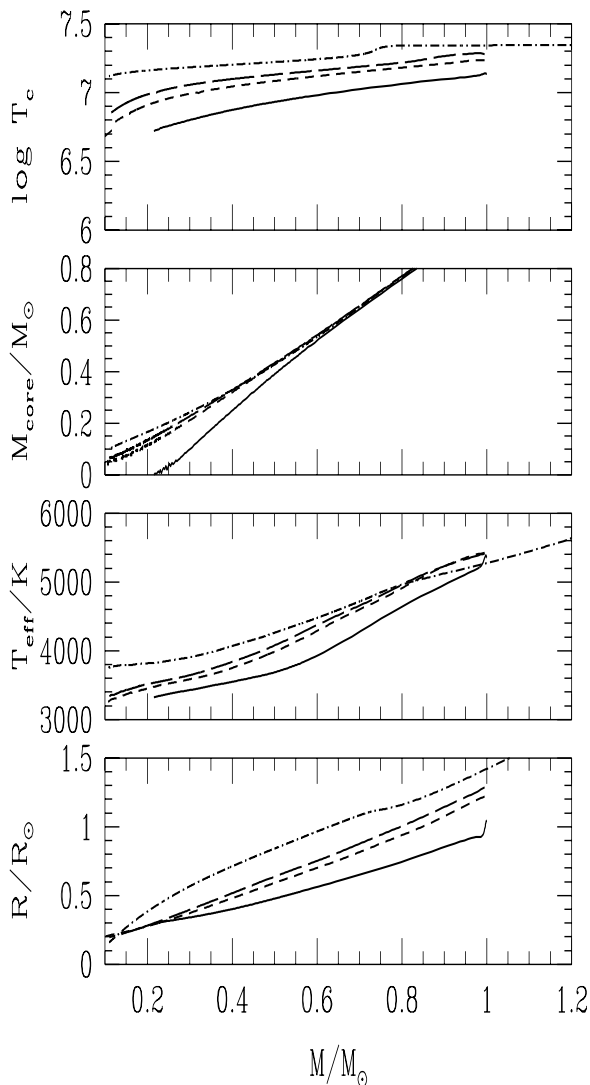


Figure 4. Variation of several stellar quantities with mass for sequences with constant mass transfer rate $\dot{M} = 1.5 \times 10^{-9} M_{\odot} \text{yr}^{-1}$, initial masses $M_2 = 1$ and $1.2 M_{\odot}$ and different central H abundances X_c at the time mass transfer starts. Solid curve: standard sequence with $M_2 = 1 M_{\odot}$ and $X_c = 0.7$; dashed curve: $M_2 = 1 M_{\odot}$ and $X_c = 0.16$; long-dashed curve: $M_2 = 1 M_{\odot}$ and $X_c = 0.05$; dash-dotted curve: $M_2 = 1.2 M_{\odot}$ and $X_c = 0.05$. M_{core} is the mass of the radiative core. T_c is the central temperature (in K).

a band with spectral types significantly later than ZAMS stars at the same orbital period.

Our calculations tested if the observed spectral types can be reproduced by varying two main parameters, the mass transfer rate \dot{M} (assumed constant), and the degree of nuclear evolution of the secondary before mass transfer starts (measured in terms of the initial central H fraction X_c). Only CVs forming with massive ($\gtrsim 1 - 1.2 M_{\odot}$) donors, i.e. at long periods, can have donors where H is significantly depleted in the centre.

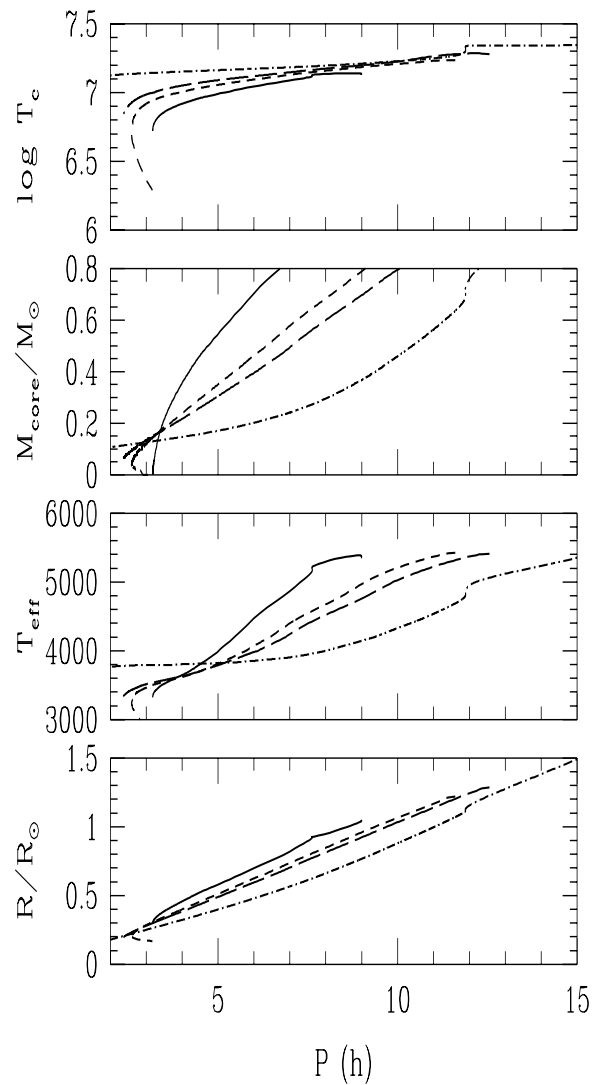


Figure 5. Same as Fig. 4, but as a function of orbital period.

We summarize our results as follows: (i) In the framework of the standard discontinuous orbital braking model for the period gap, the observed gap between 2-3 h is well reproduced by sequences starting from ZAMS donors and proceeding at a mass transfer rate $\dot{M} \sim 1 - 2 \times 10^{-9} M_{\odot} \text{yr}^{-1}$ near the upper edge of the gap. (ii) Higher transfer rates ($\dot{M} \gtrsim 5 \times 10^{-9} M_{\odot} \text{yr}^{-1}$) than assumed in (i) near the upper edge of the gap are required to explain the full range of late spectral types of secondaries in CVs with periods $P = 3 - 6$ h. This is true whatever the evolutionary state of the donor at turn-on of mass transfer. (iii) A family of evolutionary sequences starting mass transfer from an evolved donor with varying $X_c < 0.5$ and low mass transfer rate ($\dot{M} \lesssim 5 \times 10^{-9} M_{\odot} \text{yr}^{-1}$) covers the observed locations of CVs in the P -SpT diagram for $P \gtrsim 6$ h. (iv) For these sequences, higher mass transfer rates than in (i) are required

Table 2. Characteristic quantities as a function of P (for $3 \leq P/h \leq 10$) for sequences with initial donor mass $M_2 = 1$ or $1.2 M_\odot$, constant mass transfer rate $\dot{M} = 1.5 \times 10^{-9} M_\odot \text{yr}^{-1}$ and different central H abundance X_c at the time mass transfer starts.

M_2 M_\odot	X_c	P h	M M_\odot	SpT	T_{eff} K	R R_\odot
1.00	0.700	9.0	1.000	G5-G6	5360.	1.0441
		8.0	0.992	G6	5289.	0.9454
		7.0	0.870	K0-K1	4870.	0.8205
		6.0	0.751	K4-K5	4467.	0.6972
		5.0	0.616	M0-M1	3979.	0.5758
		4.0	0.475	M2-M3	3648.	0.4574
		3.5	0.377	M3	3521.	0.3856
1.00	0.550	9.0	0.976	G6	5276.	0.9933
		8.0	0.912	G8	5105.	0.9111
		7.0	0.795	K1-K2	4713.	0.7784
		6.0	0.684	K6	4293.	0.6666
		5.0	0.571	M1	3905.	0.5626
		4.0	0.437	M2-M3	3632.	0.4433
		3.0	0.191	M4	3324.	0.2764
1.00	0.160	10.0	0.891	G7	5201.	1.0617
		9.0	0.815	G9-K0	4961.	0.9571
		8.0	0.724	K2-K3	4672.	0.8456
		7.0	0.629	K5-K6	4385.	0.7324
		6.0	0.530	M0-M1	4071.	0.6239
		5.0	0.427	M1-M2	3809.	0.5104
		4.0	0.325	M2-M3	3619.	0.3998
		3.0	0.209	M3-M4	3464.	0.2848
1.00	0.050	10.0	0.820	G8-G9	5025.	1.0309
		9.0	0.735	K1-K2	4756.	0.9215
		8.0	0.649	K4	4516.	0.8113
		7.0	0.554	K7	4232.	0.7000
		6.0	0.463	M1	3981.	0.5941
		5.0	0.376	M1-M2	3789.	0.4884
		4.0	0.288	M2-M3	3627.	0.3820
		3.0	0.199	M3	3514.	0.2800
1.20	0.050	10.0	0.531	K6	4329.	0.8796
		9.0	0.441	K7-M0	4145.	0.7668
		8.0	0.362	M1	3999.	0.6613
		7.0	0.299	M2	3905.	0.5655
		6.0	0.248	M2	3853.	0.4785
		5.0	0.206	M2	3821.	0.3969
		4.0	0.172	M1-M2	3805.	0.3221
		3.0	0.143	M1-M2	3791.	0.2509

near 3 h, otherwise they would evolve into the period gap and predict too early spectral types at shorter P .

If \dot{M} is sufficiently large, the sequences reach their minimum period above the upper edge of the period gap. The donor becomes fully convective at a mass smaller than the canonical $0.21 M_\odot$ of the standard (unevolved) sequence, but at a period longer than 3 h. If the system detaches at this point and the donor can re-establish thermal equilibrium, then mass transfer would resume at a period well below 2 h. This guarantees consistency with the standard discontinuous orbital braking model.

Points (ii) to (iv) show that if the mass transfer rate increases significantly along the secular evolution of evolved

donors, these sequences can explain the observed scatter in the P -SpT diagram *both above* 6 h, through the effect a lower X_c has on the evolutionary track (see §3 and Fig. 3), *and below* 6 h, through the effect of a higher \dot{M} (see §2 and Fig. 1).

A large range of the secular mean mass transfer rate, as suggested by (ii), could be reconciled with the sharp boundaries of the observed period gap. In the standard model these are a result of the dominance of sequences with the canonical value $1 - 2 \times 10^{-9} M_\odot \text{yr}^{-1}$ at periods close to 3 h. The apparent scatter of data in the P -SpT diagram does not support this dominance. Reasonably sharp boundaries could be maintained if the canonical value is the minimum \dot{M} value of the range of transfer rates. The observed gap edges would then be defined by this minimum mass transfer rate sequence. Sequences with higher \dot{M} would bounce before they reach the upper edge of the gap. They detach at longer periods and reattach at shorter periods than the standard sequence.

A more serious problem is that the large \dot{M} range for otherwise *similar* system parameters, as suggested by (ii) for unevolved sequences, leaves the nature of the main control parameter determining the strength of orbital angular momentum losses completely undetermined. Our experiments show that X_c could be this parameter.

The full observed range of data in the P -SpT diagram could be explained if the orbital braking strength increases both with decreasing P and decreasing X_c . This ensures that period bounce prevents evolved sequences from overpopulating the period gap, while they still pass through rather late spectral types at long periods. The resulting \dot{J} law must give the canonical value of \dot{M} at 3 h for $X_c = 0.7$. A large \dot{M} range for unevolved systems is not required.

With standard magnetic braking laws (e.g. by Verbunt & Zwaan 1981, Mestel & Spruit 1987) the transfer rate usually increases with period, and is smaller for sequences with more evolved donors (see e.g. Pylyser & Savonije 1989, Singer et al. 1993, Ritter 1994), i.e. has just the opposite differential behaviour than the one we propose. Given the significant uncertainty in these magnetic braking models and our poor knowledge of the underlying stellar magnetic dynamo, the suggestion that observations favour a non-standard law does not appear unrealistic. Further considerations of the theory of magnetic braking to assess our finding are clearly beyond the scope of this paper. We note, however, that there are magnetic braking scenarios in the literature that lead to an increase of \dot{M} with progressing evolution. Kolb & Ritter (1992) obtained this for a Verbunt & Zwaan (1981)-type law when only the donor's convective envelope is coupled to the orbital motion. Zangrilli et al. (1997) found this property for their boundary-layer dynamo.

At this point we re-emphasize that the input physics on which our stellar models are based provides an excellent description of observed properties of isolated low-mass stars. Unless there are effects peculiar to CV secondaries that are not taken into account by the models (e.g., effects due to the rapid rotation, or the irradiation by the white dwarf and accretion disc), one is forced to accept that a large fraction of CVs have a nucleary evolved donor star. This is in stark contrast to predictions of standard models for the formation of CVs, where most CVs form with a secondary which is too low-mass ($\lesssim 0.6 M_\odot$) to be evolved (Politano

1996, King et al. 1994). But this predominance of unevolved donors is mainly due to the neglect of systems forming with a secondary that is significantly more massive than the white dwarf (Ritter 2000). These undergo thermal-timescale mass transfer at a rate $\gtrsim 10^{-7} M_{\odot} \text{yr}^{-1}$ and are usually associated with supersoft sources (e.g. di Stefano and Rappaport 1994). It is perfectly possible that these systems reappear as standard CVs once the mass ratio ($q = \text{donor mass}/\text{WD mass}$) is sufficiently small. In descendants of this thermal-timescale evolution any degree of nuclear evolution prior to mass transfer is possible. De Kool (1992) finds that the impact of these survivor systems depends on the assumed initial mass ratio distribution which ultimately determines the secondary mass distribution in post-common envelope binaries. For de Kool's model 1 ($dN \propto dq$) survivor systems completely dominate the CV population. A full appraisal of the viability of the apparent predominance of nuclear evolved systems is beyond the scope of our study. This requires a full population synthesis with self-consistent treatment of X_c -dependent angular momentum losses.

Finally, the accurate determination of donor masses could provide an observational test of our hypothesis that a significant fraction of CV donors is nuclearily evolved. Observational errors are still too large (e.g. Smith & Dhillon 1998) for this test. Systems with the most discrepant (late) spectral type should have the smallest mass at any given P .

Acknowledgments We are grateful to K. Beuermann, H. Ritter, H. Spruit, F. and E. Meyer for valuable discussions. We thank the referee, R. Smith, for a careful reading of the manuscript. I.B. thanks the Max-Planck-Institut für Astrophysik (Garching) and the University of Leicester for hospitality during the realization of part of this work. The calculations were performed on the T3E at Centre d'Etudes Nucléaires de Grenoble. We thank A. Norton for improving the language of the manuscript.

REFERENCES

- Allard F., Hauschildt P.H., Alexander D.R., Starrfield S. 1997, *ARA&A* 35, 137
- Baraffe I., Chabrier G. 1996, *ApJ* 461, L51
- Baraffe I., Chabrier G., Allard F., Hauschildt P.H. 1995, *ApJ* 446, L35
- Baraffe I., Chabrier G., Allard F., Hauschildt P.H. 1997, *A&A* 327, 1054
- Baraffe I., Chabrier G., Allard F., Hauschildt P.H. 1998, *A&A* 337, 403
- Beuermann K., Baraffe I., Kolb U., Weichhold, M. 1998, *A&A*, 339, 518
- Burrows A., Hubbard W.B., Saumon D., Lunine J.I. 1993, *ApJ*, 406, 158
- Chabrier G., Baraffe I. 1995, *ApJ*, 451, L29
- Chabrier G., Baraffe I. 1997, *A&A*, 327, 1039
- Chabrier G., Baraffe I. 2000, *ARA&A*, in press
- Chabrier G., Baraffe I., Plez B. 1996, *ApJ*, 459, L91
- De Kool M. 1992, *A&A*, 261, 188
- Di Stefano R., Rappaport S. 1994, *ApJ*, 437, 733
- Hameury J.M. 1991, *A&A*, 243, 419
- Hameury J.M., King A.R., Lasota J.P., Ritter H. 1988, *MNRAS*, 231, 535
- Hauschildt P.H., Allard F., Baron E. 1999, *ApJ*, 512, 377
- King A.R. 1988, *QJRAS*, 29, 1
- King A.R., Kolb U., de Kool M., Ritter H. 1994, *MNRAS*, 269, 907
- Kolb U. 1993, *A&A*, 271, 149
- Kolb U., Baraffe I. 1999, *MNRAS*, 309, 1034
- Kolb U., Ritter H. 1990, *A&A*, 236, 385
- Kolb U., Ritter H. 1992, *A&A*, 254, 213
- Kolb U., King A.R., Baraffe I., 2000, *MNRAS*, submitted
- Laughlin G., Bodenheimer P., Adams F. 1997, *ApJ*, 482, 420
- Leggett S.K., Allard F., Berriman G., Dahn C.C., Hauschildt P.H. 1996, *ApJS*, 104, 117
- Mestel L., Spruit H.C. 1987, *MNRAS*, 226, 57
- Politano M. 1996, *ApJ*, 465, 338
- Pylyser E.H.P., Savonije G. 1989, *A&A*, 208, 52
- Rappaport S., Verbunt F., Joss PC. 1983, *ApJ*, 275, 713
- Ritter H. 1994, *Mem. Soc. Astron. Italiana*, 65, 173
- Ritter H. 1996, in Wijers R.A.M.J., Davies M.B., Tout C.A., eds., *Evolutionary Processes in Binary Stars*, Kluwer, Dordrecht, p. 223
- Ritter H. 2000, in *Cataclysmic Variables: a 60th Birthday Symposium in Honour of Brian Warner*, eds. P.A. Charles, A.R. King, D. O'Donoghue, *New Astronomy Reviews*, in press
- Saumon D., Chabrier G., VanHorn H.M. 1995, *ApJS*, 99, 713
- Singer R., Kolb U., Ritter H. 1993, *AG Abstract Series*, 9, 39
- Smith D., Dhillon V. 1998, *MNRAS*, 301, 767
- Sproats L.N., Howell S.B., Mason K.O. 1996, *MNRAS*, 282, 1211
- Spruit H.C., Ritter H. 1983, *A&A*, 124, 267
- Stehle R., Ritter H., Kolb U. 1996, *MNRAS*, 279, 581
- Verbunt F., Zwaan C., 1981, *A&A*, 100, L7
- Warner B. 1995, *Cataclysmic Variable Stars*, Cambridge Astrophysics Series 28, Cambridge: CUP
- Whyte C.A., Eggleton P.P. 1980, *MNRAS*, 190, 801
- Zangrilli L., Tout C.A., Bianchini A. 1997, *MNRAS*, 289, 59